SAND96-0336C

16Th IEEE/NPSS Symposiom on Fusion Engineering
Champaign, Illinois Sept. 30-Oct. 5, 1995.

CONF-950905--34

Thermal Fatigue Behavior of US and Russian Grades of Beryllium

R.D. Watson[a], D.L. Youchison[a], D.E. Dombrowski[b], R.N. Guiniatouline[c], I.B. Kupriynov[d]
[a]Sandia National Laboratories, MS-1129, P.O. Box 5800, Albuquerque, NM 87185
[b]Brush Wellman, Inc., 17876 St. Clair Ave, Cleveland, OH 44110
[c]Efremov Institute, P.O. Box 42, St. Petersburg, Russia 189631
[d]Russian Institute of Inorganic Materials, 5 Rogov St., Moscow, 123060, Russia, Box 369

ABSTRACT

A novel technique has been used to test the relative low cycle thermal fatigue resistance of different grades of US and Russian beryllium, which is proposed as plasma facing armor for fusion reactor first wall, limiter, and divertor components. The 30 kW electron beam test system at Sandia National Laboratories was used to sweep the beam spot along one direction at 1 Hz. This produces a localized temperature "spike" of 750 °C for each pass of the beam. Large thermal stresses in excess of the yield strength are generated due to very high spot heat flux, 250 MW/m^2. Cyclic plastic strains on the order of 0.6% produced visible cracking on the heated surface in less than 3000 cycles. An *in-vacuo* fiber optic borescope was used to visually inspect the beryllium surfaces for crack initiation. Grades of US beryllium tested included: S-65C, S-65H, S-200F, S-200F-H, SR-200, I-400, extruded high purity, HIP'd spherical powder, porous beryllium (94% and 98% dense), Be/30% BeO, Be/60% BeO, and $TiBe_{12}$. Russian grades included: TGP-56, TShGT, DShG-200, and TShG-56. Both the number of cycles to crack initiation, and the depth of crack propagation, were measured. The most fatigue resistant grades were S-65C, DShG-200, TShGT, and TShG-56. Rolled sheet Be (SR-200) showed excellent crack propagation resistance in the plane of rolling, despite early formation of delamination cracks. Only one sample showed no evidence of surface melting, Extruded (T). Metallographic and chemical analyses are provided. Good agreement was found between the measured depth of cracks and a 2-D elastic-plastic finite element stress analysis.

INTRODUCTION

Beryllium is proposed as a protective armor material on plasma facing components (PFC's) for the next generation of tokamak experiments, including the International Thermonuclear Experimental Reactor (ITER). Long-pulse operation will require active cooling to maintain steady-state surface temperatures of the 5-10 mm thick armor tiles in the range of 600-800 °C. Beryllium tiles are bonded to a water cooled copper alloy heat sink to provide active cooling. Cracking of the beryllium armor should be avoided if it leads to: (1) loss of material, (2) a reduction in thermal conductivity if cracks run across the direction of heat flow, or (3) a water leak if the cracks propagate through the tile and into the copper heat sink.

In this paper, we will describe how the e-beam test facility at Sandia National Laboratories (SNL) was used to screen the relative resistance to low cycle fatigue damage on 14 US and Russian grades of beryllium and 3 other beryllium materials. This work was performed in support of the ITER technology R&D task, T-221, "Beryllium and Other Armor Materials". This new screening technique reduces the high costs associated with traditional methods of fatigue testing of beryllium at elevated temperature, especially combined thermo-mechanical fatigue testing. A more detailed version of this paper was recently published [1].

FINITE ELEMENT ANALYSIS

The test geometry is shown in Fig. 1. Fourteen tiles were stacked side-by-side so that all samples were subjected to the same heat flux history.

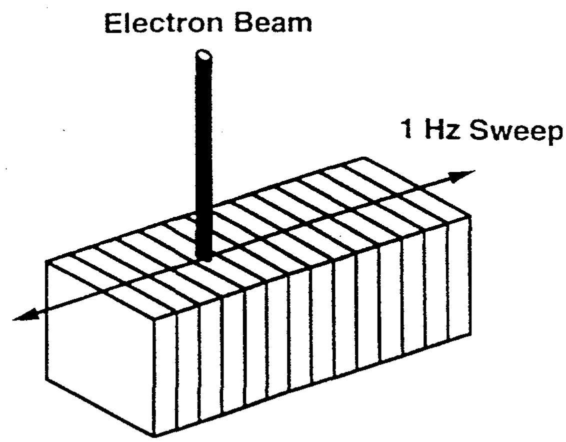

Fig. 1 Test setup showing 2 mm diameter electron beam spot swept at constant velocity across 14 tiles at 1 Hz.

A 2-D finite element mesh of the beryllium tile was generated with PATRAN, and analysed with a finite element code, ABAQUS 5.4, running on a HP 735/125 UNIX workstation. Because the tile is thin (5 mm) relative to its other dimensions (25.4 mm), a 2-D plane stress was used. First, a transient thermal analysis was performed, and then the resulting temperatures were then applied to an elastic-plastic stress analysis. The model consists of 3804 nodes and 1221 8-noded isoparametric quad elements (DC2D8 for thermal, and CPS8 for stress). A smaller mesh size was used in the region where the steepest gradients were expected, i.e. underneath the beam spot. The size of the smallest elements was 0.2 mm x 0.2

mm. Temperature-dependent thermal and mechanical properties of S-65C were used in the analysis [2].

A constant heat flux = 80 MW/m^2 was applied in ABAQUS over a 2 mm wide spot on top of the tile for a pulse length = 0.06 seconds, then turned off for 0.94 seconds. Fig. 2 shows the temperature response for a single on/off cycle at the hottest point on the surface of the beryllium tile directly underneath the beam spot. The peak temperature rises from 25 °C to 750 °C during the 0.06 heating pulse. This agrees well with experimental measurements. The hot spot has cooled back down to 35 °C at the end of the 1 s cycle, indicating that only a small amount of thermal ratcheting would occur with multiple cycles. The steep temperature profile is approximately 2 mm deep.

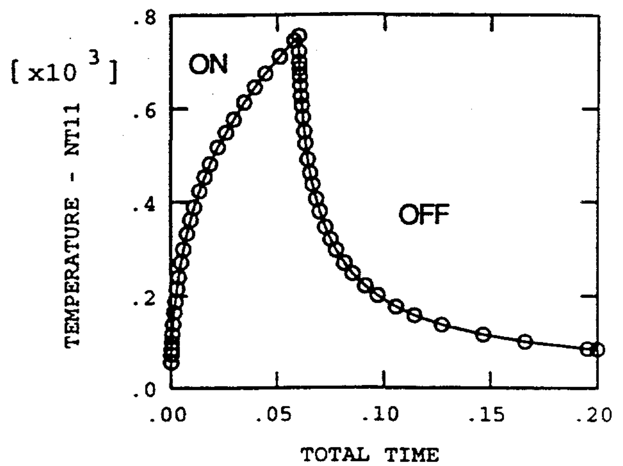

Fig. 2 Temperature (C) vs time (s) for the hottest element.

The same mesh used for the thermal analysis was subsequently used for an elastic-plastic stress analysis. A bi-linear stress/strain curve was used, with a kinematic hardening rule and temperature-dependent yield strength. Fig. 3 shows the deformed mesh plot (magnified by 200 times) at the end of the 0.06 s heating pulse.

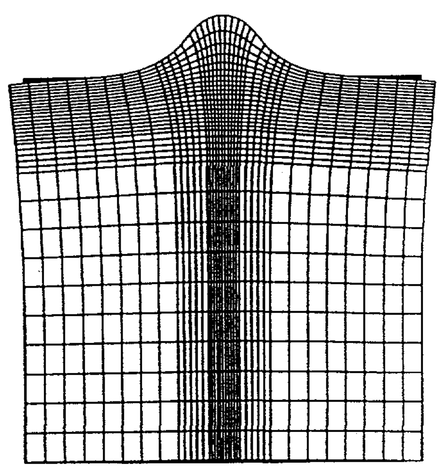

Fig. 3 Deformed ABAQUS mesh (magnified by 200 X) at the end of the heating pulse (t=0.06 s). Undeformed mesh is plotted underneath the deformed mesh.

Fig. 4 shows the X-direction stress vs plastic strain response of the hottest element underneath the beam spot for a total of 12 on/off cycles. The mechanical self-constraint of cold beryllium that surrounds the expanding hot spot creates a large compressive stress inside the hot spot during heating. The compressive stress increases rapidly up to a maximum value of -260 MPa (the yield strength) during the first 3 milliseconds when the temperature has risen about 100 °C. Then, with increasing temperature up to 750 °C, the yield strength decreases and the peak compressive stress likewise decreases to -130 MPa. Next, the heat flux is turned off, and the temperature gradient relaxes. The stress reverses sign and becomes tensile, first elastically, then plastically, as the yield strength is exceeded during cooldown. After 0.2 s, the temperature pulse has relaxed sufficiently that only small changes in the peak tensile stress (240 MPa) occur up to 1 s.

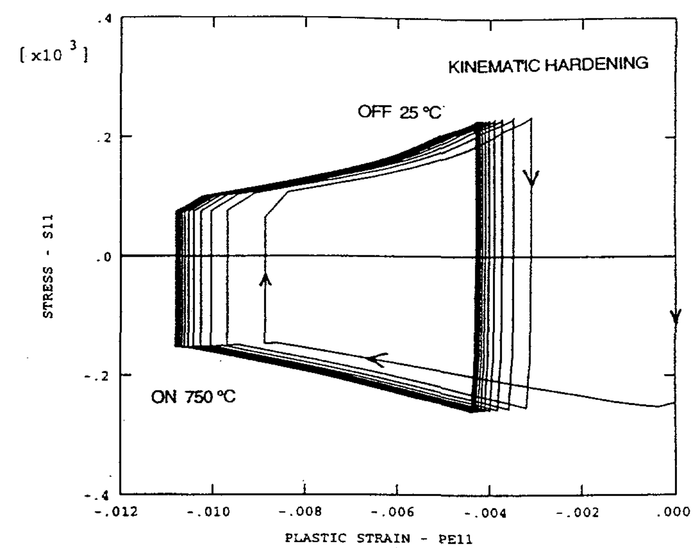

Fig. 4 Combined X-direction stress vs plastic strain for the element directly underneath the beam spot. Cyclic stress = 500 MPa and cyclic plastic strain = 0.65% after 12 cycles.

The plastic strain increases continuously up to a peak value of -0.9 % at the end of the first heating pulse. This value then decreases as the temperature pulse decays during the cooldown, leaving a permanent "residual" compressive plastic strain of -0.3% at the end of the first cycle. Shakedown to a stable response occurs during the first 6-8 cycles. The cyclic plastic strain for this element, i.e. the difference in plastic strain between the end of the heating pulse and the end of the cooling cycle, is 0.65%. Likewise, the cyclic stress is 500 MPa. The residual tensile stress at the heated surface is +240 MPa.

Fig. 5 plots the X-direction stress as a function of distance from the heated surface into the bulk at the end of the heating pulse, and at the end of the cooling cycle. The difference between these two curves is equal to the cyclic stress. The profile of cyclic stress remains rather constant for the first 1 mm, but then decays rapidly to zero at a depth of about 2 mm. This indicates that fatigue cracks, once initiated, should grow rapidly through the first 1 mm, but then slow down at they approach a depth of 2 mm. The cyclic stress range is sufficiently high, 500 MPa, that rapid crack growth would be expected.

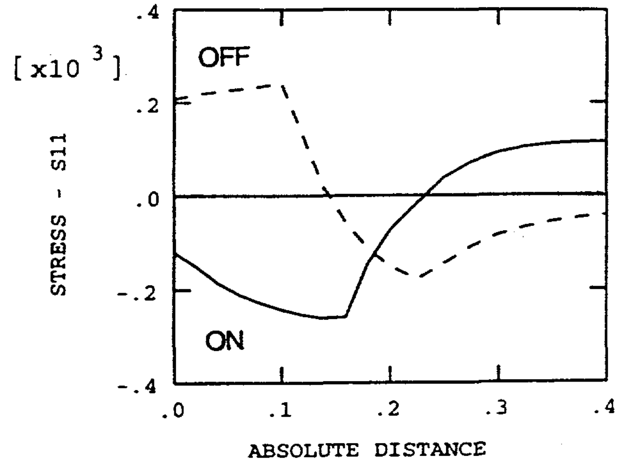

Fig. 5 Profile of X-direction stress through thickness (cm) at end of heating pulse (t=0.06 s) and end of cycle (t=1).

Fig. 6 plots the X-direction plastic strain as function of distance from the surface into the bulk at the end of the heating pulse, and at the end of the cooling cycle. The difference between these two curves is equal to the cyclic plastic strain. The profile of cyclic plastic strain decays rapidly to zero at a depth of 0.8 mm. This would indicate that fatigue crack initiation should be concentrated in a region than 0.8 mm deep. With the peak cyclic plastic strain values exceeding 0.6%, crack initiation would be expected to occur rather quickly.

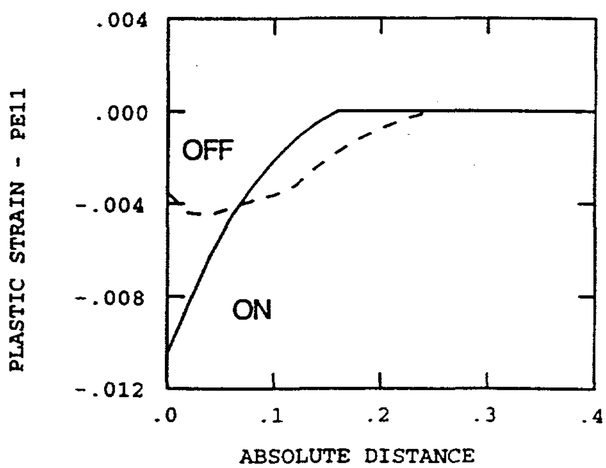

Fig. 6 Profile of X-direction plastic strain through thickness (cm) at end of heating pulse (t=0.06 s) and end of cycle (t=1).

EXPERIMENTAL PROCEDURE

Grades of US beryllium tested included: S-65C, S-65H, S-200F, S-200F-H, SR-200, I-400, extruded high purity, HIP'd spherical powder, porous beryllium (94% and 98% dense), Be/30% BeO, Be/60% BeO, and $TiBe_{12}$. Russian grades included: TGP-56, TShGT, DShG-200, and TShG-56. Each tile was 2.54 cm x 2.54 cm x 0.5 cm for the US grades, and 0.6 cm thick for the Russian grades. All of the US samples were chemically etched after machining, and degreased with an industrial grade, water based degreaser, then rinsed with acetone and methanol. Some of the Russian samples have a silvery, reflective finish which may be a the result of electropolishing. All grades typically have BeO contents on the order of 1 wt%, except I-400, which has 6 wt% BeO. The US grades showed a range of mean grain size from 5-12 microns. The mean grain size for DShG-200, 18.8 microns, is roughly twice as large as typical US grades. Also, the RF grade, TShG-56, showed an unusually large range of grain sizes, from 8 to 105 microns, within one sample.

The 30 kW Electron Beam Test System (EBTS) was used to apply a highly concentrated heat pulse to the surface of each beryllium tile. This system, described in more detail in [3], consists of a 30 kV, 1 amp (max) electron beam that can be rastered in X- and Y-directions at frequencies up to 10 kHz. For this experiment we chose to raster the beam only in one direction at a frequency of 1 Hz with a constant velocity of 8.4 cm/s over a total length of 8.4 cm. A sawtooth raster pattern was used, with a 20X faster return at the end. The tiles were clamped on both sides by water-cooled copper blocks, including a Papyex graphite paper gasket, which removed the time-averaged power deposition and prevented thermal ratcheting.

Post-test examination of the heat affected zone indicated that the beam FWHM was approximately 2 mm wide. Rapid changes in the surface due to oxidation, microcracking, and melting prevented the use of optical pyrometry for accurate surface temperature measurements. However, visual observation of the color of the hot spot, after the beam had moved on to the next tile, indicated peak temperatures of at least 600 °C. Three cases (#3, 4, and 5) were run at 1300 W gun power. Each tile was inspected after every 100 cycles with an *in-vacuo* fiber optic borescope for any evidence of cracking or melting. Cycling was then continued on all 14 tiles until the last sample of the set had cracked (no more than 3000 cycles).

EXPERIMENTAL RESULTS

There are a number of common features among the samples. Looking down on the heated surface (top view) there is a clearly defined heat affected zone (HAZ) which is usually dark brown or black, with parallel bands of lighter color. It has the appearance of heavily oxidized metal. Many of the samples have a single major crack running down the middle of the HAZ parallel to the beam path, but rolled sheet and extruded samples have major cracks perpendicular to it.

The HAZ is typically 2 mm wide. In most samples, the HAZ is wider, and the damage was more severe, on the side where the beam exited the sample. Surface melting was also observed, more so on the beam's exit side. On many samples, the tile's width is narrower in the HAZ, more on the beam exit side than on the entrance side, by as much as 0.4 mm. Some tiles that cracked perpendicular to the beam's path expanded in width, rather than contracting.

Looking perpendicular to the heated surface (side view), all samples show a elliptical-shaped discolored area underneath the beam spot, consisting of both darker and lighter bands. The sharp change in color from dark brown to a light gray may be caused by different thicknesses and morphology of the BeO layer. All samples have a raised hump 0.2-0.4 mm tall directly underneath the center of the beam path. This hump is also characterized by a network of many fine cracks.

Most samples showed evidence of surface melting. Some showed evidence of net erosion of material, especially the samples with high BeO content. Many samples show a single thin, straight crack descending from the highest point of the hump perpendicular to the heated surface. Crack depths range from 0.1 mm to 2.0 mm, with the average being about 1.0 mm. These cracks were usually deeper on the side of the tile where the beam exited the sample. A few samples showed lateral cracks running parallel to the heated surface at a depth of approximately 0.1 mm below the surface. Samples which showed no evidence of surface melting were SR-200, S-65 (T), and Extruded (T).

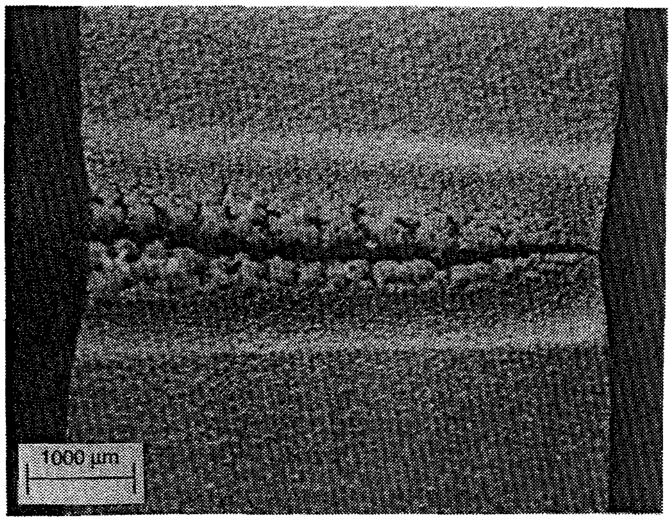

Fig. 7 Top view of S-200F after 2400 cycles. Longitudinal VHP billet orientation is parallel to heated surface. Mag 18X.

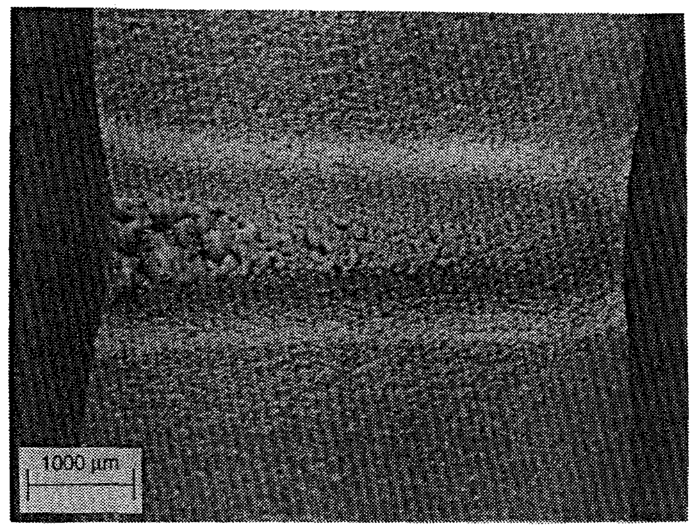

Fig. 9 Top view of S-65C after 2400 cycles. Longitudinal VHP billet orientation is parallel to heated surface. Mag 18X.

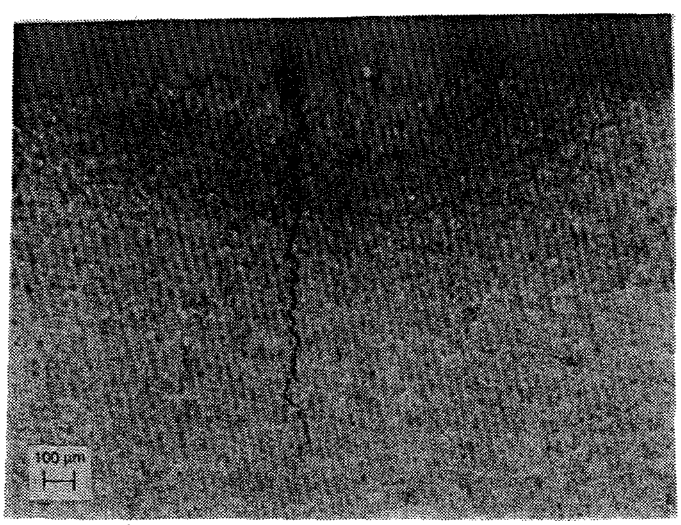

Fig. 8 Side view of S-200F after 2400 cycles. Longitudinal VHP billet orientation is parallel to heated surface. Mag 47X.

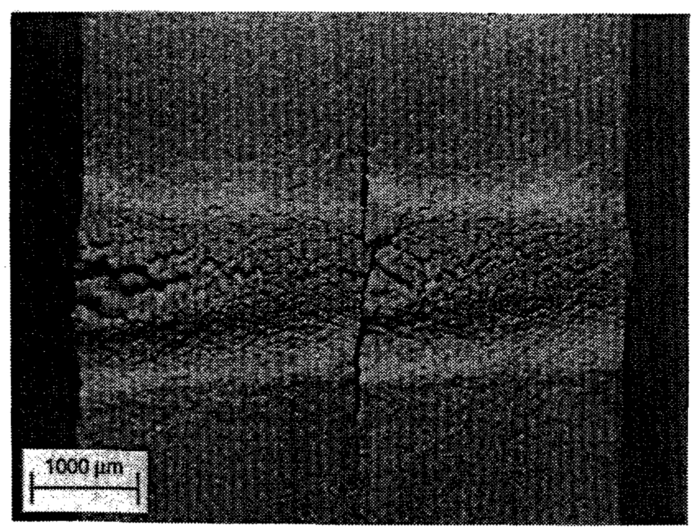

Fig. 10 Top view of SR-200 rolled sheet after 2400 cycles. Delamination crack is in the plane of rolling. Mag 18X.

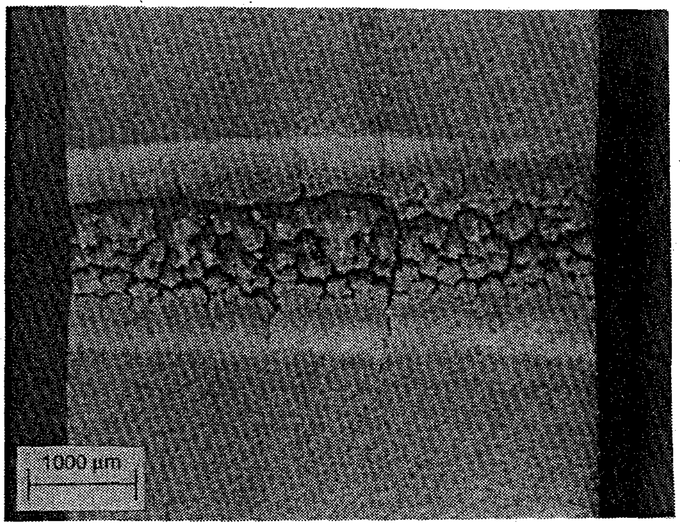

Fig. 11 Top view of I-400 after 2400 cycles. Longitudinal VHP billet orientation is parallel to heated surface. Mag 18X.

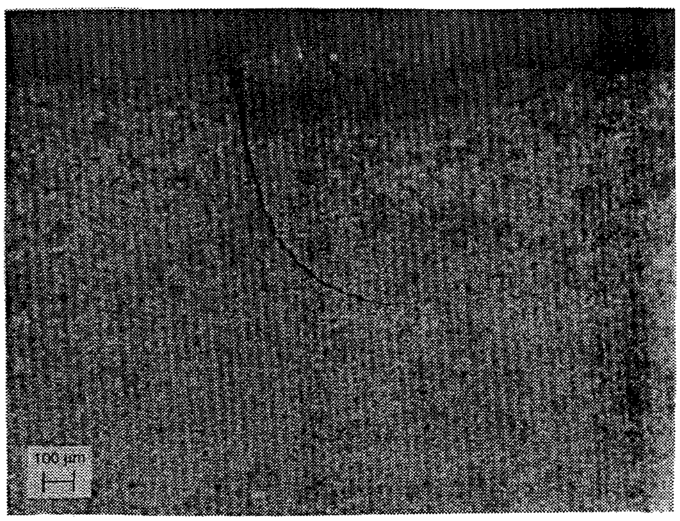

Fig. 12 Side view of I-400 after 2400 cycles. Longitudinal VHP billet orientation is parallel to heated surface. Lateral cracks can be seen running parallel to heated surface. Mag 47X.

The samples with the <u>best</u> resistance to crack initiation were: S-65C (L), DShG-200, S-65C (T), TShGT, S-65H, and TShG-56. The samples with the <u>worst</u> resistance to crack initiation were: TiBe12, Be/60wt% BeO, Be/30wt% BeO, I-400 (L), SR-200, 94% S-65. The samples with the <u>shortest</u> cracks were: SR-200, TShGT, S-65C (L), DShG-200, Be/60% BeO, and TShG-56. The samples with the <u>longest</u> cracks were: $TiBe_{12}$, Extruded (L), S-200F (L), I-400 (T) and TGP-56.

The cracks tended to fall into two categories: either straight, narrow and long or blunt, wide and short. The blunt, wide and short crack morphology was correlated with the best crack initiation resistance. Only one sample had both types of cracks: S-65C with the transverse direction parallel to the heated surface. This sample shows a long, straight, narrow crack propagation from one of the blunt cracks. There was no strong correlation with microstructural features such as grain size and inclusion concentration, but there was a complicated relationship with texture. The highly textured grades (sheet and extrusion) performed worse than partially textured grades such as VHP. HIP grades, which have minimal texture, performed worse than VHP grades. The average crack length of all the samples was 0.8 mm (excluding $TiBe_{12}$). Typically, the cracks on the beam's exit side were 20% longer than on the beam's entrance side.

DISCUSSION

Fig. 13 summarizes the experimental results; it shows both the crack initiation cycles and crack propagation depths. $TiBe_{12}$ is not shown, because the crack depths are off the scale (16 mm). If we look at just the grades of beryllium metal with isotropic and near-isotropic properties (S-65C, S-65H, S-200F, S-200F-H, 94% S-65, 98% S-65, I-400, TGP-56), we see a clear trend. Samples in this group with high number of cycles to crack initiation also have low crack propagation depths, and visa-versa. This could be because they are tougher, or simply because there haven't been many cycles <u>after</u> crack initiation to propagate cracks deeper. Likewise, samples which initiate cracks early on have more time (e.g. cycles) to grow the crack deeper.

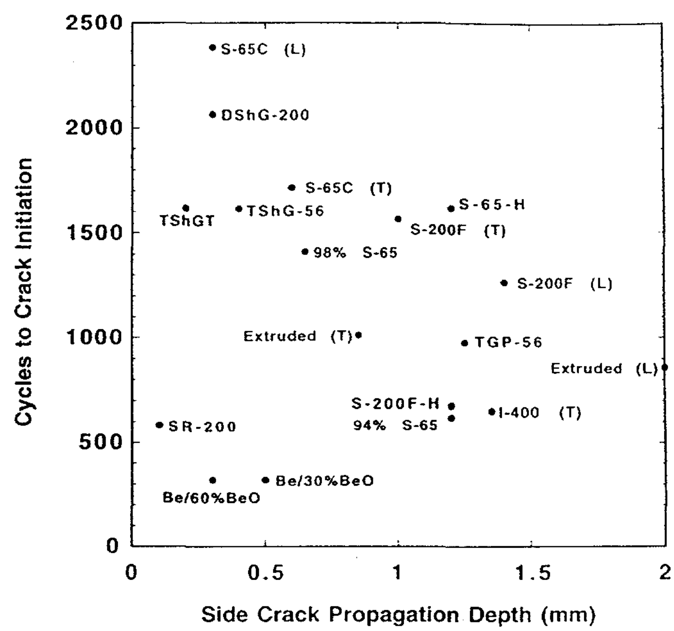

Fig. 13 Summary of experimental results. Samples with the best overall fatigue resistance are S-65C, DShG-200, TShGT, and TShG-56.

For the case of SR-200 (TShGT also), the low strength and ductility in the direction perpendicular to the plane of rolling explains why these samples formed a delamination crack relatively quickly. However, in-plane, vertical cracks (when viewed from the side), show excellent resistance to growth. This is probably due to the outstanding mechanical properties in the plane of rolling (350 MPa Yield, 550 MPa Ultimate, and 25% elongation, at room temperature for SR-200, from Table 4). Use of beryllium in this form, as sheet "lamellae", bonded to a copper tube with the tube running perpendicular to the plane of the sheet, has been proposed for ITER high heat flux components by Merola et. al. [4].

The good resistance to melting of the SR-200 and S-65 samples correlate well to the short crack depths that was observed. In the case of extruded (T) sample, the lack of melting, despite a deeper crack (1 mm), indicates that the crack was vertical and did not hinder heat conduction.

The rankings shown here are only done to illustrate the differences in ranking which can result from the two different ranking measurements. The rankings are not statistically significant. Much more data is needed to make these rankings valid because fatigue measurements generally exhibit a large amount of scatter.

CONCLUSIONS

A novel technique has been developed to rapidly and efficiently determine the relative low cycle fatigue resistance of a number of different beryllium materials. Operating the electron beam at 1 Hz produces a localized temperature spike of sufficient intensity such that cyclic plastic strains on the order of 0.6% and cyclic stresses of 500 MPa are created, producing visible cracking in less than 3000 cycles.

A number of features were correctly predicted by a 2-D elastic-plastic finite element analysis, including: peak temperatures, width of the heat affected zone, orientation of the main crack, formation of a bump on the surface, depth of crack propagation, curvature of crack near a compressive zone, and residual tensile stresses causing crack opening upon cooldown. The 2-D, plane stress model did not account for two features: (1) out-of-plane stresses that caused delamination cracks in rolled sheet beryllium, and (2) narrowing of the tile due to plastic deformation. Future efforts in finite element modeling should include: (1) using a 3-D model, with a moving e-beam spot, (2) anisotropic material's properties, (3) improved description of the yield surfaces (e.g. kinematic vs isotropic hardening).

The most fatigue resistant grades were S-65C, DShG-200, TShGT, and TShG-56. Rolled sheet Be (SR-200) and TShGT showed excellent crack propagation resistance in the plane of rolling, despite early formation of delamination cracks. Only one sample showed no evidence of surface melting, extruded (T), despite cracking. The good thermal conduction is preserved because cracks only grow perpendicular to the heated surface because of the highly aligned grain structure in the extruded form.

The degree and morphology of cracking is strongly dependent on the metallographic texture. Vacuum hot pressed grades generally perform better than hot isostatic pressed grades. Likewise for the longitudinal direction oriented parallel to the heated surface. Lower metallic impurity contents correlates well with increased fatigue resistance, but BeO content does not correlate well. The use of highly textured beryllium, i.e. rolled sheet, in the form of thin "lamellae" proposed by Merola appears to be an attractive concept for improving fatigue lifetime of high heat flux components.

A second round of electron beam experiments is recommended in order to generate better statistics, and to improve our understanding of low cycle fatigue behavior. More tests using pre-cracked or notched samples could be performed to focus only on the crack propagation aspects. Also, samples which have previously been exposed to simulated plasma disruptions (plasma guns) could be tested. Neutron-irradiated samples could be tested in the JUDITH facility. Finally, samples of plasma sprayed beryllium should be tested.

ACKNOWLEDGMENTS

This work was performed at Sandia National Laboratories, supported by the US Department of Energy, Office of Fusion Energy, under contract DE-AC04-94AL85000. The authors wish to thank Brush Wellman, Inc. for their supply of the beryllium materials, and post-test examination, metallography, and chemical analyses. We wish to also thank Fred Bauer, Ken Trancosa, Jimmie McDonald, LaWonda Wold, and Wynona Sexson for their contributions contributions to operating the electron beam test system and computer network.

REFERENCES

[1] R.D. Watson, D.L Youchison, D.E. Dombrowski, R.N. Guiniatouline, I.B. Kupriynov, "Low Cycle Thermal Fatigue Testing of Beryllium Grades for ITER Plasma Facing Components", Proc. 2nd IEA International Workshop on Beryllium Technology for Fusion, Jackson, WY, Sept, 1995.

[2] R.D. Watson and J.B. Whitley, "Thermal Fatigue Tests of a Prototype Beryllium Limiter for JET", J. Nuclear Eng. and Design, Vol. 4, p. 49, (1986).

[3] D.L. Youchison, J.M. McDonald, L.S. Wold, "High Heat Flux Testing Capabilities at Sandia National Laboratories-New Mexico", ASME Heat Transfer in High Heat Flux Systems, HTD-Vol. 301, p. 31 (1994).

[4] M. Merola, R. Matera, G. Federici, S. Chiocchio, "Thermomechanical study of a new concept for a beryllium-protected high heat flux component", Fusion Eng. and Design, Vol. 28, p. 97 (1995).

DISCLAIMER